Activation Mechanism of Retinal Rod Cyclic GMP Phosphodiesterase Probed by Fluorescein-Labeled Inhibitory Subunit†

Theodore G. Wensel*,‡ and Lubert Stryer
Department of Cell Biology, Stanford University School of Medicine, Sherman Fairchild Center, Stanford, California 94305
Received July 20, 1989; Revised Manuscript Received October 13, 1989

ABSTRACT: The cyclic GMP phosphodiesterase (PDE) of vertebrate retinal rod outer segments (ROS) is kept inactive in the dark by its γ subunits and is activated following illumination by the GTP form of the α subunit of transducin (T_α–GTP). Recent studies have shown that the stoichiometry of the inhibited holoenzyme is $\alpha\beta\gamma_2$. T_α–GTP and γ act reciprocally. We have investigated the activation mechanism using fluorescein-labeled γ subunit (γ^F) as a probe. γ^F containing a single covalently attached fluorescein was prepared by reaction of PDE with 5-(iodoacetamido)fluorescein and purification by reversed-phase high-pressure liquid chromatography (HPLC). γ^F, like native γ, inhibits the catalytic activity of trypsin-activated PDE and transducin-activated PDE. Inhibition by γ^F was overcome by further addition of T_α–GTP. γ^F binds very weakly to ROS membranes stripped of PDE and other peripheral membrane proteins. γ^F added to ROS membranes became incorporated into a component that could be extracted with a low ionic strength buffer. HPLC gel filtration showed that γ^F became part of the PDE holoenzyme. Incorporation occurred in less than 1 min in the presence of light and GTP, but much more slowly ($t_{1/2} \sim 500$ s) in the absence of GTP. This result indicates that transducin activates PDE by binding to the holoenzyme and accelerating the dissociation of γ from the inhibitory sites. The binding of γ^F to trypsin-activated $PDE_{\alpha\beta}$ was monitored by steady-state emission anisotropy measurements and compared with PDE activity. The results indicate that occupancy of each γ binding site suppresses about half of the total activity of $PDE_{\alpha\beta}$; the dissociation constants for these sites are similar ($\sim$10 pM). Our results fit a simple model in which T_α–GTP interacts first with an $\alpha\beta\gamma\gamma$ holoenzyme and carries away one of the γ subunits, to form a partially active $PDE_{\alpha\beta\gamma}$ complex. This complex can then be converted to fully active $PDE_{\alpha\beta}$ when a second γ subunit is carried away by another T_α–GTP. The T_α–PDE_γ complex stays bound to the membrane.

In vertebrate photoreceptors, the biochemical event that converts the light signal (photoisomerization of rhodopsin) into an electrical signal (closing of cation channels in the plasma membrane) is the rapid hydrolysis of cGMP (Fesenko et al., 1985; Yau et al., 1986; Cote et al., 1986; Blazynski & Cohen, 1986; Zimmerman et al., 1985). Photoexcited rhodopsin (R*) activates the α subunit of transducin by catalyzing the formation of the GTP-bound form, T_α–GTP (Fung & Stryer, 1981). T_α–GTP, in turn, switches on the phosphodiesterase (PDE), which catalyzes the hydrolysis of cGMP (Fung et al., 1981). PDE and transducin are both peripheral membrane proteins (Kühn, 1981). Activation occurs on the membrane surface (Liebman & Sitaramayya, 1984; Tyminski & O'Brien, 1984; Wensel & Stryer, 1988). PDE consists of three kinds of subunits: α (85 kDa), β (82 kDa), and γ (9.7 kDa) (Baehr et al., 1979). The catalytic unit is $\alpha\beta$, whereas γ is inhibitory (Hurley & Stryer, 1982). T_α–GTP acts by removing the inhibitory constraint imposed by γ. We previously reported that γ binds to native PDE with a dissociation constant on the order of 10^{-11} M and that nanomolar γ can reverse the activation of PDE by micromolar T_α–GTPγS (Wensel & Stryer, 1986).

Four simple models for the activation process are shown in Figure 1. In each, T_α–GTP (denoted by T) binds first to the PDE holoenzyme. It has recently been shown that the holoenzyme contains two inhibitory subunits (i.e., $\alpha\beta\gamma\gamma$; Deterre et al., 1988), but for simplicity only one γ subunit is depicted here. In model 1, T carries γ away from the $\alpha\beta$ catalytic subunit of PDE, whereas in model 2 T stays bound to $\alpha\beta$ and displaces γ. T–γ leaves the membrane in model 1b, and γ leaves the membrane in model 2b. In contrast, T forms a complex with $\alpha\beta\gamma$ in models 3 and 4, which differ in that γ is taken away from its original site in model 4, but not in model 3. The reported release of inhibitor from activated amphibian ROS (Yamazaki et al., 1983) supports model 1b or 2b. However, for bovine ROS, γ remains tightly bound to activated ROS membranes (Wensel & Stryer, 1986; Deterre et al. 1986), which rules out models 1b and 2b. Models 1a, 3, and 4 are consistent with the finding that a T–γ complex can be released from activated bovine ROS by washing with a low ionic strength buffer (Deterre et al., 1986). Models 3 and 4 were favored by the finding that trypsin-activated PDE ($\alpha\beta$) had a different K_m for cGMP and a different affinity for γ than did PDE in activated ROS (Sitaramayya et al., 1986). In contrast, models 3 and 4 are ruled out by our previous finding that T and γ act reciprocally in controlling PDE activity.

Additional complexity is introduced by the presence of two γ subunits in the PDE holoenzyme; it has been suggested that differential activities of PDE with one, two, or no γ subunits bound may play an important role in the physiological processes of activation and inactivation (Deterre et al., 1988). It has recently been reported that the γ displays cooperative binding to PDE and that transducin acts cooperatively to activate PDE as well (Whalen & Bitensky, 1989). It has also recently been proposed (Bennett & Clerc, 1989) that PDE has a high-affinity site for T_α–GTP that induces partial activation and a low-affinity site that induces maximal activation.

It is evident that the mechanism of activation of PDE by transducin is an open question despite intensive study by several laboratories. The problem is especially challenging because

† This work was supported by Research Grant EY02005 to L.S. and National Research Service Award EY05815 to T.W.
‡ Present address: Department of Biochemistry, Baylor College of Medicine, One Baylor Plaza, Houston, TX 77030.

0006-2960/90/0429-2155$02.50/0

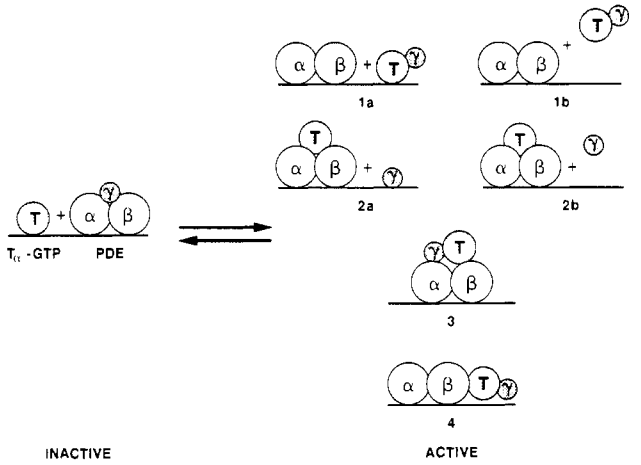

FIGURE 1: Models for the activation by PDE by transducin. T denotes the activated form of transducin (T_α–GTP), α, β, and γ denote the subunits of PDE, and the horizontal line represents the surface of the disk membrane. In model 1, γ forms a complex with T which dissociates from PDE. In model 2, T displaces γ from PDE. In model 3, T binds to a complex of all three subunits of PDE and alters their interactions to switch on catalytic activity. In model 4, T binds to PDE and causes γ to move away from its inhibitory site; γ remains associated with the T–PDE complex.

all of the PDE subunits stay bound to the membrane. Transducin activates PDE in solution only very weakly. It therefore seemed desirable to develop assays for subunit interactions that use physical methods (rather than enzymatic activity measurements) to report directly on binding events in intact ROS membranes. We have prepared an active fluorescein-labeled derivative of the γ subunit of PDE to probe the activation process. We report here the preparation, purification, and characterization of this probe and its incorporation into PDE under activating conditions. Our results support model 1a (Figure 1) or a formally equivalent model in which the initial inactive state is $PDE_{\alpha\beta\gamma\gamma}$ (Deterre et al., 1988) and in which sequential removal by T of two γ subunits from independent binding sites forms $\alpha\beta\gamma$ and $\alpha\beta$ complexes with half and full activity, respectively.

Materials and Methods

Reagents. 5-(Iodoacetamido)fluorescein was obtained from Molecular Probes. GTP and GTPγS were obtained from Boehringer-Mannheim.

Buffers. Buffer A (moderate salt buffer) contained 10 mM MOPS [3-(*N*-morpholino)propanesulfonic acid] adjusted to pH 7.4 with NaOH, 60 mM NaCl, 30 mM KCl, 2 mM $MgCl_2$, 1 mM dithiothreitol, 0.02% NaN_3, and 0.1 mM phenylmethanesulfonyl fluoride (PMSF). Buffer B (gel filtration buffer) contained 20 mM MOPS, pH 7.2 (adjusted with KOH), 2 mM $MgCl_2$, 0.5 mM sodium EDTA, 0.02% NaN_3, 2 mM 2-mercaptoethanol, and 0.1 mM PMSF and 0.1 M NaCl.

ROS and Protein Preparations. ROS were prepared from frozen bovine retinas (J. A. Lawson Co., Lincoln, NE), and transducin was purified as described (Fung & Stryer, 1980; Fung et al., 1981). PDE was prepared by hydroxylapatite chromatography (Wensel & Stryer, 1986). Bleached ROS membranes (190 mg of rhodopsin, obtained from 400 retinas) were extracted with moderate salt (buffer A) and then low-salt buffers (5 mM Tris-HCl, pH 7.4, 0.5 mM $MgCl_2$, 1 mM DTT, 0.1 mM PMSF) as described to obtain 8.7 mg of low-salt-extracted proteins. The solution was adjusted to 30 mM sodium phosphate, pH 7.2, and 50 mM NaCl and applied to a 1.5 cm × 10 cm column of hydroxylapatite. PDE was eluted with a linear gradient (420 mL total, flow rate of 0.49 mL/min) from 30 M sodium phosphate, pH 7.2, to 0.3 M phosphate (2:1 Na^+:K^+, pH 7.2). Trypsin-activated PDE and T_α–GTPγS were prepared as described (Wensel & Stryer, 1986). ROS membranes stripped of peripheral proteins (urea-stripped ROS membranes) were prepared by washing with 4 M urea (Yamanaka et al., 1985). In some cases, the urea-stripped membranes were prepared with bleached ROS, and 11-*cis*-retinal was added in the dark to regenerate rhodopsin.

Electrophoresis. SDS–polyacrylamide gel electrophoresis was performed by using the method of Laemmli (1970) with the resolving gel containing a linear gradient from 6% to 20% polyacrylamide.

Assays. PDE assays were carried out by using the pH recording method (Liebman & Evanczuk, 1982) with an initial cGMP concentration of 2 mM or by monitoring hydrolysis of [^{3}H]cGMP (Wensel & Stryer, 1986) with an initial cGMP concentration of 2.4 mM. Inhibitory activity of γ^F was determined by titration of trypsin-activated PDE (Wensel & Stryer, 1986).

Preparation of γ^F. 5-(Iodoacetamido)fluorescein (1.0 mM) was mixed with PDE (1.8 μM) in sodium phosphate buffer (50 mM, pH 7.2) in the dark at 23 °C. To determine the time course of the reaction, aliquots were removed during the reaction and mixed first with 2-mercaptoethanol (to 50 mM) and then with trichloroacetic acid (10%). The precipitated protein was sedimented, washed with acetone, and analyzed by SDS–polyacrylamide gel electrophoresis. The γ bands on the gel were either visualized and photographed on an ultraviolet transilluminator or cut out and soaked in 0.1% SDS to elute γ^F for measurement of fluorescence. The γ band was labeled maximally within 10 min under these conditions. The effect of exhaustive labeling was determined by allowing the reaction to proceed for 3 h at 23 °C and then assaying for PDE activity before and after limited trypsin digestion. To test for the specificity of the reaction, PDE was oxidized by treatment with dithiodipyridyl before addition of (iodoacetamido)-fluorescein, and the extent of labeling was compared to that observed with PDE that had been previously treated with DTT (5 mM).

Purification of γ^F by Reversed-Phase HPLC. After the reaction was stopped by addition of mercaptoethanol, unincorporated dye was removed by repeated dilution (to 2 mL) and reconcentration (to ~20 μL) using a Centricon 30 apparatus. This dilution–concentration cycle was repeated five times. The concentrated protein was suspended in 15% (v/v) acetonitrile containing 0.1% trifluoroacetic acid (HPLC start buffer), heated to 60 °C, and spun in a Beckman airfuge at 30 psi for 10 min to remove precipitated PDE subunits, primarily α and β. The supernatant was applied to an Alltech Macrosphere C4 column and eluted with a gradient from 15% to 65% acetonitrile (0.1% trifluoroacetic acid throughout). Fractions of 1 mL were collected in siliconized polypropylene tubes. The fluorescence of an aliquot of each fraction was measured after it was diluted into a solution containing 0.1% SDS and 1 N NaOH. Inhibitory activity was assayed by vacuum drying 1 μL of each fraction, adding a solution of trypsin-activated PDE, and measuring the resultant PDE activity. Absorbance was monitored at 280 and 440 nm. An injection of the 2-mercaptoethanol conjugate of 5-(iodoacetamido)fluorescein was used as a standard to quantitate the amount of fluorescein in the γ^F peak.

Fluorescence Measurements. Corrected emission and excitation spectra were measured by using an SLM 8000 con-

trolled by an IBM PC. Samples were excited at 490 nm, and the emission was monitored at 520 nm.

Emission Anisotropy Measurements. The binding of γ^F to PDE was monitored by observing changes in emission anisotropy of the attached fluorescein chromophore. The SLM 8000 instrument was used with the following modifications: fluorescence was excited with the 476.5-nm line of a vertically polarized argon ion laser passed through a Glan-Thompson polarizing prism. Emission at 540 nm (selected with 540-nm interference filters and Corion LL500 dielectric film cut-on filters) was detected simultaneously by two photomultipliers equipped with Glan-Thompson polarizers oriented to detect either horizontally or vertically polarized light. The relative sensitivity of the detection system to light of horizontal and vertical polarization was determined by rotating the excitation polarizer 90° (the laser emits ~1% residual horizontally polarized light) and recording the intensity detected by each detector. Alternatively, the 488-nm line of the laser was used to excite the isotropic emission of Tb(III)EDTA$^-$ at 546 nm, and the intensity was detected by each detector recorded.

γ^F Uptake Assays. The extent of rapid uptake of γ^F by ROS membranes was assessed by mixing ROS (7.6 μM R*) with γ^F (4 nM) in the presence or absence of GTP (20 μM) in buffer A. After 3 min at room temperature, the suspension was placed on ice and then centrifuged in an airfuge (5 min, 30 psi). The binding of γ^F to membranes was determined by measuring the loss of fluorescence from the supernatant. Following moderate salt washing, pellets were washed with an equal volume of distilled water to remove PDE and other low-salt-extractable proteins, and the fluorescence of this low-salt supernatant was also measured. The fluorescence of γ^F that had not been mixed with ROS was not measurably affected by changes in ionic strength. In each case, the background fluorescence from samples devoid of γ^F was subtracted from the total fluorescence.

Kinetics of γ^F Uptake by ROS. ROS membranes 2.5 μM R*) were added to tubes containing dried γ^F (50 nM final concentration) in the presence or absence of GTP (0.1 mM). PDE in this reaction mixture was estimated to be 10 nM. At various times, aliquots were removed and the membranes sedimented in an airfuge (30 psi). The fluorescence of the supernatant solutions and of the resuspended pellets was measured.

HPLC Gel Filtration Analysis of Bound γ^F. γ^F was incorporated into ROS membranes by incubating γ^F (6 nM) with ROS (67 μM R*) in buffer A, with or without GTP (35 μM) for 30 min at 23 °C. The suspension was diluted by addition of an equal volume of buffer B and sedimented in an airfuge (5 min, 30 psi). The supernatant solution containing free γ^F was removed, and the washed pellets were resuspended in a buffer identical with buffer B except for the absence of NaCl. This suspension was diluted 4-fold with 2 mM $MgCl_2$ to elute PDE and other low-salt-extractable proteins. This suspension (38 μM R*) was spun for 5 min at 30 psi (airfuge). The composition of the supernatant solution was adjusted to that of buffer B by addition of a 10-fold concentrated stock and centrifuged again to remove traces of ROS membranes. The low-salt-extracted proteins were then concentrated to 100 μL by using a Centricon 30 membrane and injected onto a TSK 4000SW gel filtration column equilibrated with buffer B. The proteins were eluted with buffer B at a flow rate of 1 mL/min and collected in 1-mL fractions. The column was calibrated with a series of protein standards including purified PDE holoenzyme and transducin. Fractions were assayed for fluorescence as described above and for PDE activity following trypsin treatment by using the pH recording method.

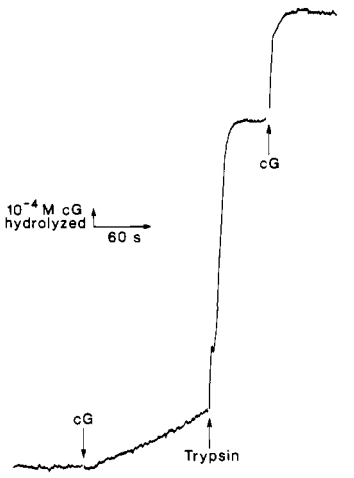

FIGURE 2: Retention of activity by both the inhibitory (γ) and the catalytic ($\alpha\beta$) subunits after extensive 5-(iodoacetamido)fluorescein labeling of PDE. After PDE was treated for 3 h with 5-(iodoacetamido)fluorescein as described in the text, the enzymatic activity of an aliquot (28 nM PDE) was assayed by the pH recording technique. At the time indicated by the leftmost arrow (cG), 2 mM cGMP was added. A very low level of hydrolytic activity was observed, as in the native enzyme. When trypsin was added to destroy the γ subunit, activation to the level expected for unlabeled PDE was observed, confirming that $\alpha\beta$ retained their catalytic activity and that γ retained its inhibitory activity. Activity prior to trypsin treatment was 2% of the trypsin-activated level (calculated from the maximal slopes of the pH record before and after trypsin treatment).

RESULTS

5-(Iodoacetamido)fluorescein Labels PDE without Altering Its Activity. The γ subunit of PDE was rapidly labeled by 5-(iodoacetamido)fluorescein, with the reaction essentially complete within 5 min. The α and β subunits were also labeled but with slower kinetics; the extent of fluorescein incorporation into α and β increased over the entire 3-h incubation period. The labeling reactions were blocked by prior oxidation using 4,4′-dithiodipyridine, indicating that the SH groups of cysteine residues were the primary targets for this reagent. Faint labeling of all three subunits in oxidized PDE was observed after long incubation times (i.e., >1 h) with the fluorescein reagent, presumably due to a much slower side reaction with lysine residues. After 3 h at 23 °C, PDE remained inactive but was fully activated upon treatment with trypsin (Figure 2). Thus, the labeling of the single sulfhydryl group in the γ subunit (Cys 68; Ovchinnikov et al., 1986) does not diminish its ability to inhibit PDE. Likewise, extensive labeling of the α and β subunits with this reagent did not decrease their catalytic activity. Similar experiments with other sulfhydryl-labeling reagents [5-[[2-((iodoacetyl)amino)ethyl]-amino]naphthalene-1-sulfonic acid, fluorescein 5-maleimide, and [^{14}C]-*N*-ethylmaleimide] yielded similar results.

Purification of γ^F by Reversed-Phase HPLC. Previously published procedures for obtaining active γ included gel filtration in acid (Hurley & Stryer, 1982), which gave low yields, heat treatment (Wensel & Stryer, 1986; Hurley & Stryer, 1982; Dummler & Etingof, 1976), which resulted in either low yields or contamination by catalytic subunits, and elution from SDS gels (Wensel & Stryer, 1986), which results in contamination with gel components. To purify γ^F, we made use of the recent finding (Brown & Stryer, 1989) that γ retains activity after purification by reversed-phase HPLC (Figure 3). Because the HPLC buffer contains only volatile components, highly purified γ^F can be obtained. The peak γ^F fraction contained 530 nM fluorescein (on the basis of 440-nm

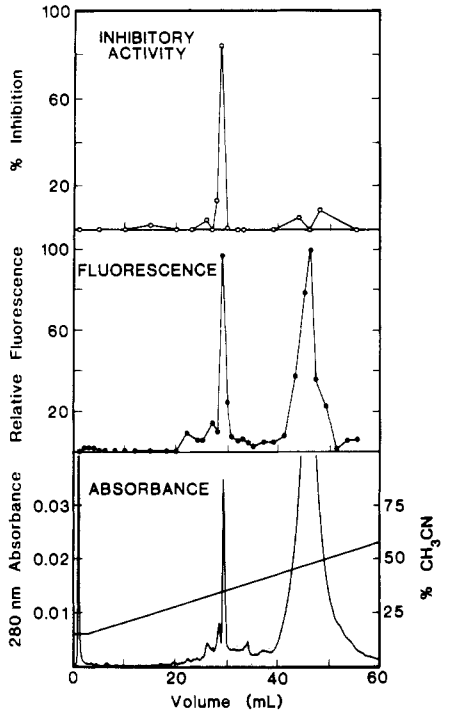

FIGURE 3: Purification of γ^F by reversed-phase HPLC. PDE labeled with 5-(iodoacetamido)fluorescein was applied to a C4 column and eluted with a gradient from 15% to 65% CH_3CN (0.1% TFA throughout).

absorbance), and 540 nM γ [(on the basis of inhibition of trypsin-activated PDE, assuming a hydrolytic rate of 4200 cGMP s^{-1} (Hurley & Stryer, 1982)]. Thus, γ^F contained a single attached fluorescein.

Purified γ^F Reversibly Inhibits PDE. Two important characteristics of the inhibitory constraint imposed on PDE by native γ are its removal by tryptic digestion and its reversal by activated transducin. Purified γ^F was tested for these properties. As shown in Figure 4, γ^F has the following properties: (1) it inhibits trypsin-activated PDE; (2) it loses its inhibitory activity upon trypsin treatment; (3) it inhibits PDE in ROS activated by light and GTPγS; and (4) its inhibitory action is reversed by addition of exogenous transducin.

GTP Enhances γ^F Uptake by a Low-Salt-Extractable Component of Light-Activated ROS. When γ^F was incubated with illuminated ROS in the presence of GTP, a significant change in fluorescence intensity was not observed (over the sum of γ^F fluorescence without membranes and membrane background). When the membranes were centrifuged in moderate salt (buffer A) 52% of the γ^F bound to the membranes. In the absence of GTP, 9.4% of the γ^F was incorporated. Washing the GTP-treated membrane pellet with low salt (a step known to remove PDE) removed 67% of the bound γ^F. Repeated moderate salt washing, on the other hand, did not remove γ^F from these membranes. In contrast, urea-stripped ROS membranes (from which PDE and other peripheral proteins have been removed) bind γ^F (and native γ) very weakly in either low or moderate salt, irrespective of the presence of GTP (data not shown). Free γ^F and bound γ^F have essentially the same emission spectrum. Hence, it was necessary to separate membranes from supernatants to determine the extent of binding.

HPLC Gel Filtration Shows That γ^F Is Incorporated Exclusively into PDE. To determine whether γ^F was in fact incorporated into PDE, a low-salt extract of γ^F-containing ROS was analyzed by gel filtration (Figure 5). The major fluorescent component coelutes from this column with PDE

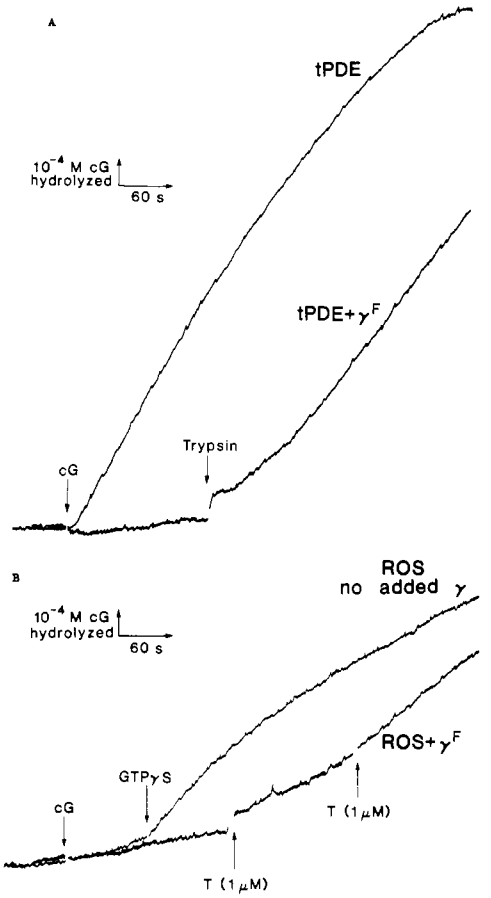

FIGURE 4: Reversibility of PDE inhibition by γ^F. (A) Trypsin-activated PDE (tPDE, 2.5 nM) was assayed in the presence (lower trace) or absence (upper trace) of γ^F (4 nM). PDE inhibited by γ^F became catalytically active when trypsin was added (to 0.1 mg/mL) at the indicated time. (B) PDE in ROS activated by light and GTPγS. ROS membranes were exposed to light, and their PDE activity was measured by the pH method at a concentration of 1 μM R* before and after addition of GTPγS (25 μM). When γ^F (26 nM) was mixed with ROS and GTPγS before addition of cGMP (lower trace), very little cGMP hydrolysis was observed after GTPγS addition. At the times indicated by arrows, aliquots of purified transducin (T) were added (final concentration 2 μM), resulting in markedly increased PDE activity.

($\sim$185 kDa) and not with γ (9.7 kDa) or with other major components of ROS. When γ^F was incubated with ROS without GTP, the fluorescence coeluted with PDE, indicating that γ^F was incorporated into PDE in that case as well; the integrated intensity of the HPLC fluorescence peak was 53% of that observed with GTP.

GTP Accelerates the Rate of Exchange of γ^F with Native γ. Over the course of several incorporation experiments in which different incubation times were used, it was observed that the extent of γ^F incorporation into ROS with and without GTP differed much more in short incubations than in long ones. A study of the kinetics of incorporation on a time scale of minutes (Figure 6) revealed the reason. When GTP was present, γ^F became incorporated into PDE in less than 1 min, the time resolution of our experiment. In contrast, exchange occurred with a half-time of about 500 s when GTP was absent. Thus, GTP (almost certainly acting through T_α-GTP) greatly accelerated the rate of γ–γ^F exchange. In addition to a faster incorporation of γ^F, the maximal incorporation in the presence of GTP was somewhat higher; this difference suggests that there may be a small pool of γ^F binding sites on PDE not accessible in the absence of GTP.

Anisotropy of γ^F Is Increased by Binding to PDE. Figure 7 shows the record of a titration of γ^F with trypsin-activated

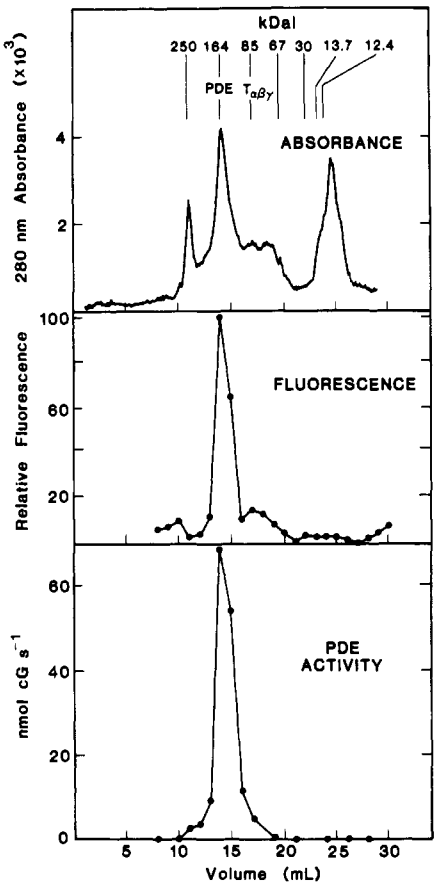

FIGURE 5: Gel filtration analysis showing γ^F incorporation into PDE. γ^F was incorporated into ROS membranes in the presence of GTP as described in the text. The membranes were washed first with moderate salt (buffer A) and then with low-salt buffer to remove PDE. The low-salt extract was concentrated and injected onto a TSK 4000 HPLC gel filtration column. Fractions were assayed for PDE activity by the pH method, and fluorescence emission was measured at 520 nm with 490-nm excitation. The elution volumes of the following standards are indicated: catalase (250 kDa, coelutes with blue dextran); PDE (184 kDa); transducin (85 kDa); BSA (67 kDa); carbonic anhydrase (30 kDa); ribonuclease A (13.7 kDa); cytochrome *c* (12.4 kDa).

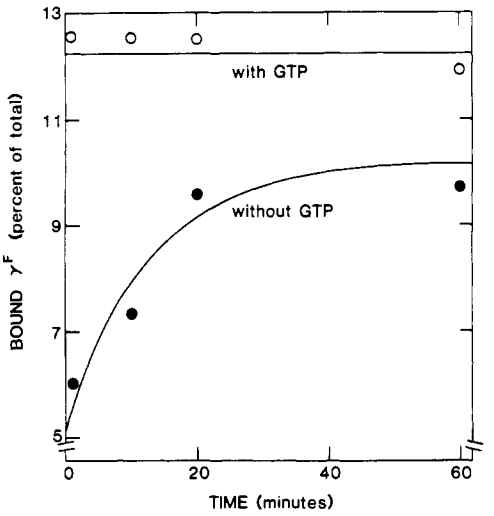

FIGURE 6: Kinetics of γ^F incorporation into PDE bound to ROS membranes. ROS membranes (2.5 μM R*, approximately 10 nM PDE) were added to tubes containing dried γ^F (50 nM final concentration) in the presence or absence of GTP (0.1 mM). At the indicated times, aliquots were removed and the membranes sedimented in an airfuge (30 psi). The fluorescence of the supernatant solutions and of the resuspended pellets was measured (490-nm excitation, 520-nm emission). The fluorescence intensity of the pellets is plotted as a percentage of the sum of the fluorescence intensity of the pellets and the supernatants. The curve shown is calculated for a background of 5.2% (corresponding to approximately 5 μL of the solution retained in the pellet from each 100-μL sample), a maximum incorporation of 10.2%, and a first-order rate constant for uptake of 1.3×10^3 s^{-1}. Theoretical maximal incorporation, assuming equal affinities of γ and γ^F for PDE, is 16.7%.

PDE ($PDE_{\alpha\beta}$). As increasing amounts of $PDE_{\alpha\beta}$ were added, the anisotropy (A) increased from its initial value (A_f) of 0.14, characteristic of free γ^F, to a maximal value (A_b) of 0.23, characteristic of γ^F bound to PDE. This signal serves as a measure of the fraction of γ^F in a sample that is bound to PDE (f_b), according to $f_b = (A - A_f)/(A_b - A_f)$.

Correlation of γ^F Binding with Inhibition. The lower panel of Figure 8 shows PDE activity (determined by using the pH method) measured in samples containing 4.5 nM trypsin-activated PDE and varying amounts of γ^F. The upper panel shows the fraction of PDE sites occupied (f), determined from emission anisotropy measurements at each γ concentration according to $f = f_b\gamma_0/P_0$, where γ_0 and P_0 are the total added γ and total PDE, respectively. At lower γ^F concentrations, the activity decreased in a nearly linear fashion with increasing γ^F, with activity eventually reduced to an undetectably low level. The binding curve almost exactly mirrors the inhibition curve, with f, the fraction of γ sites occupied, increasing linearly at low γ concentrations and approaching saturation at values above 9 nM.

Discussion

We have prepared a fully functional fluorescent derivative of the inhibitory subunit of retinal rod cGMP phosphodiesterase. γ^F, like native γ, inhibits the catalytic activity of PDE; this inhibition is overcome by the addition of activated transducin or trypsin. The single fluorescein in γ^F is attached via a sulfhydryl-specific reaction and therefore must be attached to cysteine 68, the sole thiol in the polypeptide (Ovchinnikov et al., 1986). The availability of this fluorescent subunit facilitates probing the activation mechanism by directly monitoring its interactions with membranes and other subunits. γ^F binds very weakly to disk membranes stripped of PDE and other peripheral membrane proteins. In contrast, γ^F was taken up by PDE bound to membranes, most likely by exchange of γ^F for native γ in the holoenzyme. Incorporation of γ^F was markedly accelerated by T_α–GTP. Thus, transducin induces the dissociation of γ from its binding site on the holoenzyme.

These findings, taken together with previous studies, provide insight into the mechanism of PDE activation. In model 2a (Figure 1), activated transducin displaces γ from PDE; the released γ stays tightly bound to the membrane. Our finding that γ binds only weakly to the membrane excludes model 2a. In model 1a, T_α–GTP carries γ away from PDE and forms a membrane-bound complex with γ. This model is supported by the finding that a complex of T_α–GTPγS and γ can be released from disk membranes by washing them with a low ionic strength buffer (Deterre et al., 1986). Models 1b and 2b, in which γ is released from the membrane during the activation process, were ruled out previously by SDS–polyacrylamide gel analyses showing very little γ in supernatants of GTPγS-activated ROS that were centrifuged (Wensel & Stryer, 1986; Deterre et al., 1987). Likewise, repeated washing of activated membranes did not yield a pellet containing permanently activated PDE. Our finding that activated transducin markedly accelerates the incorporation of γ^F into PDE (Figure 6) excludes model 3, in which γ is presumed not to leave its binding site on PDE during activation. Models 3 and 4 are also inconsistent with the finding that PDE activity is reciprocally controlled by γ and T_α–GTP (Wensel & Stryer,

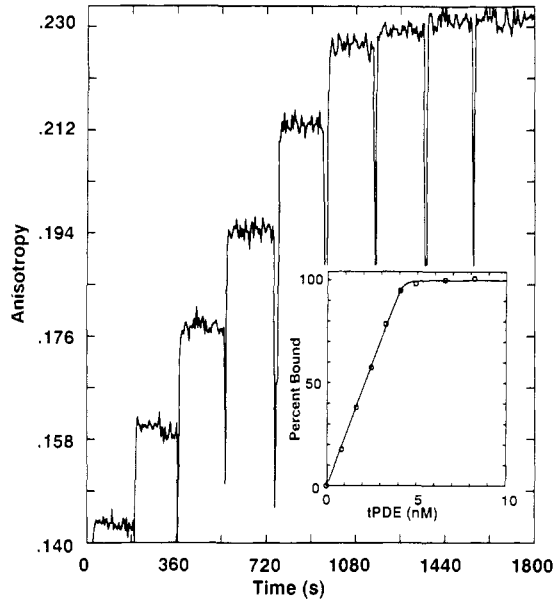

FIGURE 7: Anisotropy of γ^F as a function of added trypsin-activated PDE. The emission anisotropy of γ^F (8.7 nM) was monitored continuously while aliquots of trypsin-activated PDE were added to the stirred 1.5-mL sample. The large vertical spikes mark PDE additions. The first six PDE additions were 2 μL each, and each increased the total PDE by 0.82 nM. The final two additions were 4 μL each, resulting in total PDE concentrations of 6.6 and 8.2 nM, respectively. Emission of γ^F at 540 nm was excited by a vertically polarized laser beam (476.7 nm) and monitored simultaneously by two photomultipliers fitted with polarizing prisms oriented vertically (F_v) or horizontally (F_h). Anisotropy was calculated according to $A = (gF_v - F_h)/(gF_v + 2F_h)$, where $g = F_h/F_v$ measured with horizontally polarized excitation. Background fluorescence, measured with a buffer blank containing PDE and no γ^F, made a negligible contribution to the total signal. The total emission intensity of γ^F ($F_v + 2F_h$) was not measurably changed by the addition of tPDE. The inset shows the percent of γ^F bound to tPDE ($100f_b$), calculated as described in the text by using the anisotropy data and plotted as a function of added trypsin-activated PDE (tPDE).

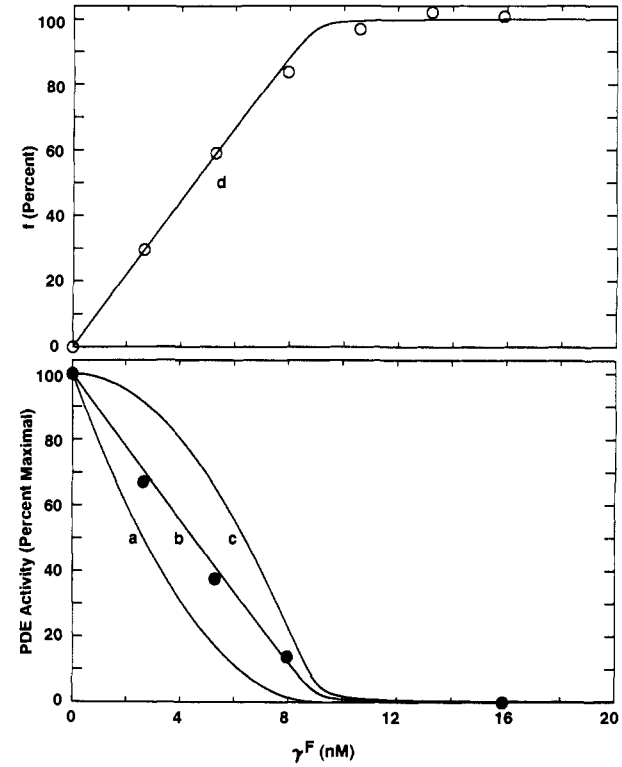

FIGURE 8: Titration of trypsin-activated PDE with γ^F. Both the catalytic activity and γ^F emission anisotropy were measured as a function of γ^F added to trypsin-activated PDE (4.5 nM). The experimental points in the upper panel (open circles) were obtained from anisotropy measurements, which report on the binding of γ^F, and are plotted as the fractional occupancy, f, of the γ binding sites on PDE. The solid circles in the lower panel depict PDE activity, which was determined from the hydrolysis of cGMP. The following assumptions about the activity of different PDE–γ complexes were used to calculate the theoretical curves a–c: curve a, $\alpha\beta$ fully active, $\alpha\beta\gamma\gamma$ and $\alpha\beta\gamma$ completely inactive; curve b, $\alpha\beta\gamma$ half-active, $\alpha\beta$ fully active, $\alpha\beta\gamma\gamma$ completely inactive; curve c, $\alpha\beta\gamma$ and $\alpha\beta$ fully active, $\alpha\beta\gamma\gamma$ inactive. The binding curve d and curves a–c were all calculated by assuming a K_d of 10 pM and two γ binding sites per PDE.

1986). Model 3 cannot account for the inhibition of transducin-activated PDE by the addition of exogenous γ. Model 4 predicts that the addition of a second equivalent of γ should lead to inhibition that cannot be reversed by subsequent addition of T_α–GTPγS, contrary to what is found experimentally.

Thus, the evidence strongly favors model 1a. However, this simple picture must now be modified to take into account the recent finding that PDE holoenzyme contains two γ subunits ($\alpha\beta\gamma\gamma$) instead of one ($\alpha\beta\gamma$) (Deterre et al., 1988). An activation scheme that incorporates this finding is shown in Figure 9. Two new questions are posed by the existence of two γ binding sites: (1) What are the relative activities of $\alpha\beta\gamma\gamma$, T–$\alpha\beta\gamma\gamma$, T–$\alpha\beta\gamma$, $\alpha\beta\gamma$, and $\alpha\beta$? (2) What are the equilibrium and kinetic constants connecting these states?

Our experiments with trypsin-activated PDE and γ^F shed light on the relative activity levels of $\alpha\beta\gamma\gamma$, $\alpha\beta\gamma$, and $\alpha\beta$, as well as on the equilibrium constants for association of γ with these two complexes. Our finding that inhibition of catalytic activity parallels the binding of γ (Figure 8) suggests that the binding of each γ subunit inhibits about half of the total activity. Thus, $\alpha\beta\gamma\gamma$ has almost no activity (<1% of $\alpha\beta$), whereas $\alpha\beta\gamma$ has 50% of the activity of $\alpha\beta$. To illustrate this point, Figure 8 depicts theoretical curves predicted by two contrasting models. In the first, $\alpha\beta\gamma\gamma$ and $\alpha\beta\gamma$ are assumed to be inactive (i.e., binding of one γ subunit inhibits completely), whereas in the second $\alpha\beta$ and $\alpha\beta\gamma$ are assumed to be equally active (i.e., both γ subunits must bind for any inhibition to occur). In both cases it is assumed that the two binding sites have equal affinities, and both dissociation constants are on the order of 10 pM (Wensel & Stryer, 1986). This assumption is consistent with the shape of the experimental titration curves, which indicate nearly stoichiometric binding over most of the titrations. In this simple case, the fraction of PDE in each of the three states $\alpha\beta$, $\alpha\beta\gamma$, and $\alpha\beta\gamma\gamma$ can be calculated from the binomial distribution given the fraction of PDE's γ sites that are occupied, f: $[\alpha\beta]/P_0 = (1-f)^2$; $[\alpha\beta\gamma]/P_0 = 2f(1-f)$; $[\alpha\beta\gamma\gamma]/P_0 = f^2$. The fraction

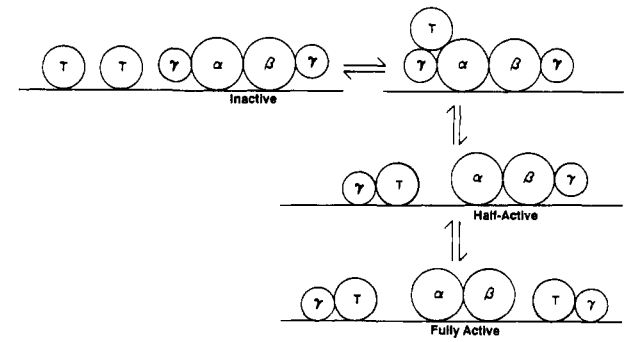

FIGURE 9: Model for activation of PDE by transducin. Symbols for subunits are as in Figure 1. The inactive (dark) form of PDE is assumed to be $\alpha\beta\gamma\gamma$. T (T_α–GTP) binds to this complex, forming T–$\alpha\beta\gamma\gamma$. T–γ dissociates from this complex and stays bound to the membrane, leaving T–$\alpha\beta\gamma$. A second molecule of T can react with $\alpha\beta\gamma$ to give T–$\alpha\beta\gamma$ and then dissociate to form a second membrane-bound T–γ complex.

of occupied γ binding sites can in turn be calculated from the total PDE, P_0, the total γ^F, γ_0, and the dissociation constant, K_d according to $f = 1/(2P_0)[\gamma_0 - (-b + (b^2 + 4\gamma_0 K_d)^{1/2})/2]$, where $b = K_d - \gamma_0 + 2P_0$. Figure 8 shows the result expected for each model; curve a, calculated for the case where binding of a single γ results in complete inhibition, displays marked curvature and is concave upward, whereas curve c, calculated for the case where binding of two γ subunits is necessary for inhibition (i.e., where $\alpha\beta\gamma$ is fully active), displays a similar degree of curvature but is concave downward. These models are clearly inconsistent with the data. In contrast, curve b, predicted for the case where $\alpha\beta\gamma$ has half the activity of $\alpha\beta$, is linear over most of the titration and is consistent with the data. The binding curve, d, does not depend on the activity levels of the different states but does depend on the assumed number of sites, the concentration of added γ^F, and the assumed K_d. The agreement of the data with the curve predicted by using the same parameters used to generate curves a–c (i.e., curve d) confirms that the estimates of total number of γ binding sites (two per PDE), the γ^F concentration, and K_d (10 pM) are reasonable and that errors in these parameters cannot account for the discrepancy between the data and curves a and c.

The simplest model consistent with the data, then, is the one shown in Figure 9, which is formally equivalent to model 1a (Figure 1). Two molecules of T must interact with each PDE to form $\alpha\beta$ and fully activate the PDE. However, the intermediate state, $\alpha\beta\gamma$, is also active, with a catalytic activity about half that of $\alpha\beta$.

We do not know whether T–$\alpha\beta\gamma\gamma$ or T–$\alpha\beta\gamma$ is active or how much of each is present at equilibrium. However, the γ^F exchange kinetics point to a central role for a T–$\alpha\beta\gamma\gamma$ complex in either case. T cannot accelerate the dissociation of γ from holo-PDE without first binding to the $\alpha\beta\gamma\gamma$ complex. Thus, T–$\alpha\beta\gamma\gamma$ must be the first intermediate formed in the activation reaction.

The model depicted in Figure 9 can serve as a working hypothesis to guide further experiments aimed at elucidating the activation mechanism. Direct measurements of subunit interactions (e.g., using fluorescence energy transfer and other techniques) will be important in testing this model and in elucidating the activation mechanism and the structures of the intermediates. The methods described here for preparing functional PDE specifically labeled in the γ subunit, and potentially with different labels on each of two γ subunits, should facilitate these experiments.

References

Baehr, W., Devlin, M. J., & Applebury, M. L. (1979) *J. Biol. Chem. 254*, 11669–11677.

Bennett, N., & Clerc, A. (1989) *Biochemistry 28*, 7418–7424.

Blazynski, C., & Cohen, A. I. (1986) *J. Biol. Chem. 261*, 14142–14147.

Brown, R. L., & Stryer, L. (1989) *Proc. Natl. Acad. Sci. U.S.A. 86*, 4922–4926.

Cote, R. H., Nicol, G. D., Burke, S. A., & Bownds, M. D. (1986) *J. Biol. Chem. 261*, 12965–12975.

Deterre, P., Bigay, J., Robert, M., Pfister, C., Kühn, H., & Chabre, M. (1986) *Proteins: Struct. Funct. Genet. 1*, 188–193.

Deterre, P., Bigay, J., Forquet, F., Robert, M., & Chabre, M. (1988) *Proc. Natl. Acad. Sci. U.S.A. 85*, 2424–2428.

Dummler, I. L., & Etingof, R. N. (1976) *Biochim. Biophys. Acta 429*, 474–484.

Fesenko, E. E., Kolesnikov, S. S., & Lyubarsky, A. L. (1985) *Nature 313*, 310–313.

Fung, B. K.-K., & Stryer, L. (1980) *Proc. Natl. Acad. Sci. U.S.A. 77*, 2500–2504.

Fung, B. K.-K., Hurley, J. B., & Stryer, L. (1981) *Proc. Natl. Acad. Sci. U.S.A. 78*, 152–156.

Goldberg, N. D., Ames, A., III, Glander, J. E., & Walseth, T. F. (1983) *J. Biol. Chem. 258*, 9213–9219.

Griswold-Prenner, I., Young, J. H., Yamane, H. K., & Fung, B. K.-K. (1988) *Invest. Ophthamal. Vis. Sci. 29*, 219.

Haugland, R. P. (1985) *Handbook of Fluorescent Probes and Research Chemicals*, pp 13–15, Molecular Probes Inc., Junction City, OR.

Hurley, J. B., & Stryer, L. (1982) *J. Biol. Chem. 257*, 11094–11099.

Kühn, H. (1981) *Curr. Top. Membr. Transp. 15*, 171–201.

Liebman, P. A., & Evanczuk, T. (1982) *Methods Enzymol. 81*, 532–542.

Liebman, P. A., & Sitaramayya, A. (1984) *Adv. Cyclic Nucleotide Protein Phosphorylation Res. 17*, 215–225.

Means, G., & Feeney, R. A. (1971) *Chemical Modifications of Proteins* pp 105–110, Holden-Day San Francisco.

Nakatani, K., & Yau, K.-W. (1985) *Biophys. J. 47*, 356.

Ovchinnikov, Yu. A., Lipkin, V. M., Kumarev, V. P., Gubanov, V. V., Khramtsov, N. V., Akhmedov, N. B., Zagranichny, V. E., & Muradov, K. G. (1986) *FEBS Lett. 204*, 288–292.

Sitaramayya, A., Harkness, J., Parkes, J. H., Gonzalez-Oliva, C., & Liebman, P. A. (1986) *Biochemistry 25*, 651–656.

Thompson, W. J., & Appleman, M. M. (1971) *Biochemistry 10*, 311–316.

Tyminski, P. N., & O'Brien, D. F. (1984) *Biochemistry 23*, 3986–3993.

Wensel, T. G., & Stryer, L. (1986) *Proteins: Struct. Funct. Genet. 1*, 90–99.

Wensel, T. G., & Stryer, L. (1988) in *Enzyme Dynamics and Regulation* (Chock et al., Eds.) Springer-Verlag, New York pp 102–112.

Whalen, M. M., & Bitensky, M. W. (1989) *Biochem. J. 259*, 13–19.

Yamazaki, A., Stein, P. J., Chernoff, N., & Bitensky, M. W. (1983) *J. Biol. Chem. 258*, 8188–8194.

Yau, K.-W., Haynes, L. W., & Nakatani, K. (1986) *Fortschr. Zool. 33*, 343–366.

Zimmerman, A. L., Yamanaka, G., Eckstein, F., Baylor, D. A., & Stryer, L. (1985) *Proc. Natl. Acad. Sci. U.S.A. 82*, 8813–8817.